

University of Nebraska - Lincoln

DigitalCommons@University of Nebraska - Lincoln

---

Virology Papers

Virology, Nebraska Center for

---

2022

## Expanding Mouse-Adapted Yamagata-like Influenza B Viruses in Eggs Enhances In Vivo Lethality in BALB/c Mice

Matthew J. Pekarek

Erika M. Petro-Turnquist

Adam Rubrum

Richard J. Webby

Eric A. Weaver

Follow this and additional works at: <https://digitalcommons.unl.edu/virologypub>



Part of the [Biological Phenomena](#), [Cell Phenomena](#), and [Immunity Commons](#), [Cell and Developmental Biology Commons](#), [Genetics and Genomics Commons](#), [Infectious Disease Commons](#), [Medical Immunology Commons](#), [Medical Pathology Commons](#), and the [Virology Commons](#)

---

This Article is brought to you for free and open access by the Virology, Nebraska Center for at DigitalCommons@University of Nebraska - Lincoln. It has been accepted for inclusion in Virology Papers by an authorized administrator of DigitalCommons@University of Nebraska - Lincoln.

## Article

# Expanding Mouse-Adapted Yamagata-like Influenza B Viruses in Eggs Enhances In Vivo Lethality in BALB/c Mice

Matthew J. Pekarek <sup>1</sup>, Erika M. Petro-Turnquist <sup>1</sup>, Adam Rubrum <sup>2</sup>, Richard J. Webby <sup>2</sup> and Eric A. Weaver <sup>1,\*</sup>

<sup>1</sup> Nebraska Center for Virology, School of Biological Sciences, University of Nebraska-Lincoln, Lincoln, NE 68583, USA; mpekarek2@huskers.unl.edu (M.J.P.); epetro-turnquist2@huskers.unl.edu (E.M.P.-T.)

<sup>2</sup> Department of Infectious Diseases, St. Jude Children's Research Hospital, Memphis, TN 38105, USA; adam.rubrum@stjude.org (A.R.); richard.webby@stjude.org (R.J.W.)

\* Correspondence: eweaver2@unl.edu

**Abstract:** Despite the yearly global impact of influenza B viruses (IBVs), limited host range has been a hurdle to developing a readily accessible small animal disease model for vaccine studies. Mouse-adapting IBV can produce highly pathogenic viruses through serial lung passaging in mice. Previous studies have highlighted amino acid changes throughout the viral genome correlating with increased pathogenicity, but no consensus mutations have been determined. We aimed to show that growth system can play a role in mouse-adapted IBV lethality. Two Yamagata-lineage IBVs were serially passaged 10 times in mouse lungs before expansion in embryonated eggs or Madin–Darby canine kidney cells (London line) for use in challenge studies. We observed that virus grown in embryonated eggs was significantly more lethal in mice than the same virus grown in cell culture. Ten additional serial lung passages of one strain again showed virus grown in eggs was more lethal than virus grown in cells. Additionally, no mutations in the surface glycoprotein amino acid sequences correlated to differences in lethality. Our results suggest growth system can influence lethality of mouse-adapted IBVs after serial lung passaging. Further research can highlight improved mechanisms for developing animal disease models for IBV vaccine research.



**Citation:** Pekarek, M.J.; Petro-Turnquist, E.M.; Rubrum, A.; Webby, R.J.; Weaver, E.A. Expanding Mouse-Adapted Yamagata-like Influenza B Viruses in Eggs Enhances In Vivo Lethality in BALB/c Mice. *Viruses* **2022**, *14*, 1299. <https://doi.org/10.3390/v14061299>

Academic Editors: Lillianne Ganges and Jishu Shi

Received: 23 May 2022

Accepted: 10 June 2022

Published: 14 June 2022

**Publisher's Note:** MDPI stays neutral with regard to jurisdictional claims in published maps and institutional affiliations.



**Copyright:** © 2022 by the authors. Licensee MDPI, Basel, Switzerland. This article is an open access article distributed under the terms and conditions of the Creative Commons Attribution (CC BY) license (<https://creativecommons.org/licenses/by/4.0/>).

**Keywords:** influenza B virus; mouse-adapting; growth system; embryonated eggs; hemagglutinin; neuraminidase

## 1. Introduction

Influenza viruses are respiratory pathogens that cause up to 5 million severe cases of illness annually [1]. Influenza B viruses (IBVs), whose primary reservoir is humans [2,3], are one of two types of influenza viruses that cause annual epidemics of varying severity [1]. IBVs are responsible for roughly 25% of all influenza cases on an annual basis, but seasonal epidemics can approach or even surpass influenza A viruses (IAVs) in total and severe infections [4–6]. IBVs are categorized into two antigenically and genetically distinct lineages, B/Victoria- (B/Vic) and B/Yamagata-like (B/Yam) based on the surface glycoprotein, hemagglutinin (HA). These lineages have cocirculated since the late 1970s or early 1980s [7] and both cause infections each influenza season today.

IBVs have been shown to lead to significant disease just as severe as IAVs [8,9] and often cause heightened disease burden in children [10,11]. In 2013–2014, a quadrivalent influenza vaccine was recommended for yearly influenza vaccines in the US for increased protection against IBV and is still recommended in the United States today [12]. Additionally, recent findings suggest that the two lineages are undergoing constant changes in their antigenic epitopes, and B/Vic viruses experienced major antigenic changes in the hemagglutinin around 2018 [6,13–15]. The results from clinical, epidemiological, and evolutionary research all point to the need for more attention on both molecular research and further development of novel vaccine and therapeutic technologies to protect against IBV.

Historically, influenza viruses have been grown in the allantoic fluid of embryonated eggs as the primary vaccine production strategy [16,17]. However, the discovery of Madin–Darby canine kidney (MDCK) cell susceptibility to influenza viruses [18] has further opened studies into cell-culture-based vaccines [19–21]. Today, these two methods of virus production are the most common methods for inactivated or live-attenuated vaccine development. However, IBVs are not consistently found infecting species outside humans [2,3], which then requires adaptation of the viruses to develop a disease model for *in vivo* research. Scientists have used serial lung passaging, termed mouse-adapting, of virus to study viral characteristics or to increase pathogenicity of IBVs [22–26] and IAVs [27–29] in mice. Mouse-adapted strains are valuable for vaccine and therapeutic research by causing severe infection, which can highlight differences in protection after vaccination or therapeutic delivery. However, this process is very time consuming and resource intensive. Some studies reporting the mouse-adaptation of IBVs expanded the virus to high titer in eggs [22,23]. Alternatively, many more recent reports of mouse-adapted IBVs opt to grow the viruses in MDCK cell culture after passage in mice [24–26]. Amino acid mutations from all eight viral gene segments have been associated with increased pathogenicity after mouse-adapting [23–26], but none of the observed mutations were shared across these studies. Further understanding of the characteristics leading to more lethal IBV infections in mice will provide better tools for use in IBV vaccine and therapeutic research.

In this report, we set out to determine if the growth system of mouse-adapted IBVs after serial lung passaging influences lethality in mice. We used two Yamagata-lineage viruses, B/Phuket/3073/2013 and B/Florida/4/2006, as our parent viruses due to their inclusion in previously licensed influenza vaccines. Interestingly, we found that after 10 serial lung-lung passages of both parent strains, virus expanded in eggs was more lethal in BALB/c mice than the same virus expanded in MDCK (London line) (MDCK-Ln) cell culture. This effect was also seen after additional passaging of B/Florida/4/2006, even though the additional passaging did not further increase the lethality of the virus. We further identified that the effect on lethality was not due to differences in surface glycoprotein amino acid sequence of B/Florida/4/2006 due to no observed changes in the hemagglutinin (HA) or neuraminidase (NA) protein sequence. Overall, these results show that growing mouse-adapted B/Yam strains in eggs may produce virus with higher lethality in mice than expansion in cell culture.

## 2. Materials and Methods

### 2.1. Cells and Virus Stocks

The following reagents used in this study were kindly provided by the International Reagent Resource (IRR): influenza B virus B/Phuket/3073/2013 (Phu/13) [FR-1364] and the Madin–Darby canine kidney cells, London line (MDCK-Ln) [FR-58]. The following virus was kindly provided by the Biodefense and Emerging Infectious Disease Repository (BEI): influenza B virus B/Florida/4/2006 (FL/4/06) [NR-9696]. Stock viruses obtained from IRR and BEI were used to infect the allantoic cavity 10 or 11 day-old embryonated chicken eggs (Charles River Laboratories, Wilmington, MA, USA) and incubated at 33–35 °C. Allantoic fluid was harvested 48–72 h after infection and virus was quantified through hemagglutinating units (HAU), aliquoted, and stored at –80 °C. Each virus was only subjected to one round of growth in embryonated eggs after arrival from IRR or BEI. MDCK-Ln cells were maintained in Dulbecco’s Modified Essential Medium (DMEM) (Cytiva) supplemented with 5% fetal bovine serum (FBS) and 1% penicillin/streptomycin (P/S) (Cytiva) antibiotics and incubated at 37 °C in 5% CO<sub>2</sub>.

### 2.2. Mice

The 6–8 week old female BALB/cJ mice were purchased from the Jackson Laboratory (Bar Harbor, ME, USA). Mice were housed for experiments and general care at the University of Nebraska-Lincoln (UNL) Life Science Annex on campus according to the Association for Assessment and Accreditation of Laboratory Animal Care (AAALAC) guidelines. The

protocols followed for the experiments described were approved by the UNL Institutional Animal Care and Use Committee (IACUC) project number 2158. All experiments were conducted according to the guidelines provided in the Public Health Service Animal Welfare Policy, Animal Welfare Act, the NIH Guide for the Care and Use of Laboratory Animals, and policies put forth by the UNL animal care facility staff and veterinarians.

### 2.3. Hemagglutination Assay

A total of 50  $\mu\text{L}$  sterile Dulbecco's phosphate buffered saline (DPBS) (HyClone, Logan, UT, USA) was added to rows 2–12 of a 96-well V-bottom plate (Gibco). An amount of 100  $\mu\text{L}$  of virus sample was added to row 1 in duplicate and serially diluted two-fold down the plate. In total, 50  $\mu\text{L}$  of 0.5% chicken red blood cells (cRBCs) (Lampire Biologicals, Piperville, PA, USA) were added to each well. Virus was incubated at room temperature with cRBCs for 30–45 min before reading agglutination patterns [30] in each well to determine HAU of each virus.

### 2.4. Influenza B Virus Mouse-Adaptation

Female BALB/cJ mice ( $n = 2$ ) were anesthetized i.p. with ketamine/xylazine (K/X) (92.5/7.5 mg/kg K/X) prior to infection. Mice were then infected with 20  $\mu\text{L}$  thawed allantoic fluid from one of the two parent viruses. Three days post-infection, mice were weighed and sacrificed for harvest of the lungs. Lungs were manually homogenized in DPBS and centrifuged to separate the homogenized lysate from the cellular debris. An amount of 30  $\mu\text{L}$  lung lysate from each mouse was combined for a uniform sample. In total, 20  $\mu\text{L}$  of this combined lung lysate was used to infect the next group ( $n = 2$ ) of mice to begin passage 2. This process was repeated an additional nine times to complete 10 immediate lung-lung passages (p10). For B/FL/4/06, the process was repeated using allantoic fluid from eggs infected with p10 lung lysate as the stock virus and proceeded to complete a total of 20 lung-lung passages (p20). A model summarizing the process is shown (Figure 1).

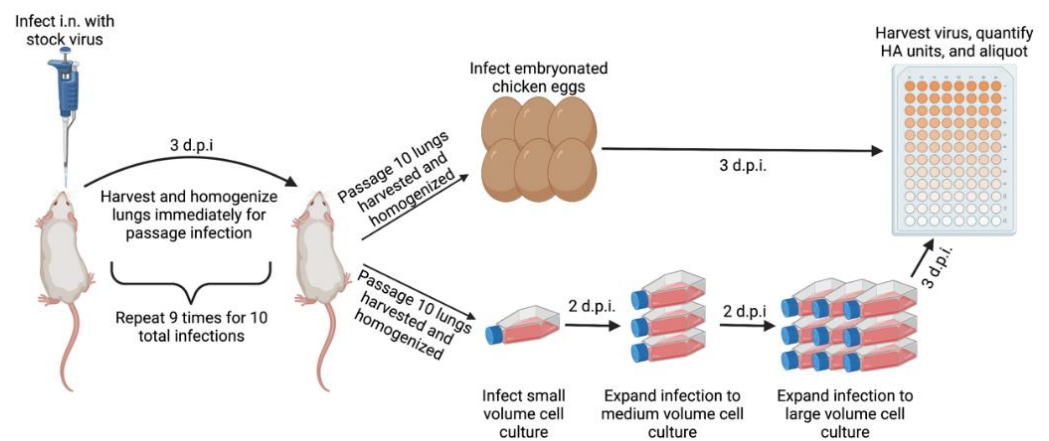


**Figure 1.** Schematic depicting mouse-passaging procedure. Passage 1 mice were infected i.n. with 20  $\mu\text{L}$  of stock virus. In 3 d.p.i., the lungs were harvested and homogenized before pooling of the lung lysate. Passage 2 mice were then infected with 20  $\mu\text{L}$  of pooled lung lysate and the procedure was repeated up to passage 10. After homogenizing passage 10 lungs, the lysate was diluted and used to infect either embryonated chicken eggs or MDCK-London cells. Infected embryonated eggs were incubated at 33  $^{\circ}\text{C}$  for 72 h before being moved to 4  $^{\circ}\text{C}$  overnight. Allantoic fluid was harvested the next day. An amount of 25  $\text{cm}^2$  infected MDCK-London cells were incubated at 33  $^{\circ}\text{C}$  for 48 h before clarified supernatant was used to infect a 75  $\text{cm}^2$  flask. The 75  $\text{cm}^2$  flask was incubated for 48 h at 33  $^{\circ}\text{C}$  before expansion into a 225  $\text{cm}^2$  flask. Finally, 225  $\text{cm}^2$  MDCK-London cells were incubated at 33  $^{\circ}\text{C}$  for 72 h before harvesting virus from supernatant. Schematic created in BioRender.

### 2.5. Mouse-Adapted Virus Growth

Lung lysate from each virus was used to infect both 10–11-day old embryonated chicken eggs and a 25 cm<sup>2</sup> tissue-culture flask (Falcon) of MDCK-Ln cells. Infected eggs were incubated at 33 °C for 72 h before being placed at 4 °C overnight. The next day, allantoic fluid from each egg was harvested and HAU were quantified before storing at –80 °C. MDCK-Ln cells in a 25 cm<sup>2</sup> flask with 2 µg/mL (0.002%) TPCK-treated trypsin in the media were infected and incubated at 33 °C with 5% CO<sub>2</sub> for 48 h. Cell supernatant was then collected and centrifuged in order to remove cell debris. The supernatant was used to then infect a 75 cm<sup>2</sup> tissue culture flask seeded with MDCK-Ln cells and incubated for 48 h 33 °C with 5% CO<sub>2</sub>. After 48 h, the supernatant was again collected and centrifuged before infecting a 225 cm<sup>2</sup> tissue culture flask of MDCK-Ln cells for 72 h before a final supernatant harvest. All strains grown in MDCK-Ln cells were verified to have an HAU ≥ 256 before harvest to ensure efficient virus production and cytopathic effects (CPE) were observed during incubation at each sequential step. Virus from both eggs and cells were quantified using HAU, aliquoted, and stored at –80 °C until future use.

### 2.6. Tissue Culture Infectious Dose (TCID<sub>50</sub>)

A total of 10 µL of virus was diluted 1:10 in the first row of a 96-well U-bottom plate. The initial dilution was then serially diluted 10-fold down the plate. An amount of  $1.5 \times 10^5$  MDCK-Ln cells in DMEM supplemented with 5% FBS without antibiotics were then added into each well and the cell-virus mixture was incubated at 33 °C with 5% CO<sub>2</sub> for 24 h. After incubation, the plate was washed twice using DPBS to remove free virus from the wells and 200 µL DMEM without FBS or antibiotics with 2 µg/mL TPCK-treated trypsin was added to all the wells. The plates were then incubated for 72 h at 33 °C with 5% CO<sub>2</sub> before adding 50 µL of 0.5% cRBCs into each well. The agglutination patterns were analyzed 45 min after addition of cRBCs [30]. TCID<sub>50</sub> values were calculated using the Reed–Muench method [31] and obtained from three independent experiments.

### 2.7. Reverse Transcription–Polymerase Chain Reaction (RT-PCR)

RNA was extracted from allantoic fluid or cell-free supernatant containing virus using the PureLink Viral RNA/DNA Mini Kit (Invitrogen, Waltham, MA, USA) by following the manufacturer's recommendations. The viral RNA was then run through qPCR using the Luna Universal Probe One-Step RT-qPCR Kit (New England Biolabs, Ipswich, MA, USA) using the Universal Influenza B Primer Probe Set (BEI Resources, Manassas, VA, USA) [NR-15608, NR-15609, NR-15610]. RT-PCR was performed using the QuantStudio 3 Real-Time PCR System (Applied Biosystems) with the following parameters: 55 °C for 30 min, 95 °C for 2 min, 95 °C for 15 s, and 60 °C for 15 s as recommended by BEI resources for the influenza virus real-time RT-PCR assay. A total of 40 cycles were used to complete amplification. IBV positive samples were identified by a Ct value difference of ≥10 cycles above the no template control reactions.

### 2.8. Influenza Challenges

Upon anesthetization with K/X, female BALB/cJ mice (n = 5) were infected with specified logTCID<sub>50</sub> unit viral challenge in a 20 µL dose. Mice were then followed for 14 days post-infection to compare weight loss between groups or humanely sacrificed upon loss of 25% initial weight. For parent virus infection (p0), allantoic fluid containing either Phu/13 or FL/4/06 was diluted 1:2 in DPBS for challenge with a 1:100 dilution of the TCID<sub>50</sub>/mL previously calculated. For mouse-adapted viruses, dilutions were calculated based off delivering 10-fold serial dilutions from 6log<sub>10</sub>TCID<sub>50</sub> to 3log<sub>10</sub>TCID<sub>50</sub> units in 20 µL doses.

### 2.9. RNA Isolation, Amplification and Sequencing

IBV RNA was generated from 200 µL of virus stock using the Qiagen RNeasy mini kit (Cat: 74104). The RNA was eluted in RNA-free water and converted to cDNA by

one-step reverse transcription and PCR using a Superscript III RT kit (Invitrogen; Cat: 12574035). Primers (10  $\mu$ M) B-HANA-UniF (5'-GGGGGGAGCAG AAGCAGAGC-3') and B-HANA-UniR (5'-CGGGTTATTAGTAGTAACAAGAGC-3'), 25  $\mu$ L reaction master mix, 16  $\mu$ L nuclease-free water, 5  $\mu$ L of RNA, and 2  $\mu$ L SSIII RT/Plat Taq was combined. cDNA was amplified using the ProFlex PCR system by Applied Biosystems. The HA and NA amplified PCR product was gel extracted using the Qiagen Gel extraction kit (Cat: 28706) and eluted in 40  $\mu$ L elution buffer. An amount of 2  $\mu$ L of cDNA was combined with 1  $\mu$ L B specific oligos (3.2  $\mu$ M) and 9  $\mu$ L water and submitted to the St. Jude Children's Research Hartwell Center for Sanger sequencing. Ab1 files received by the Hartwell center were combined and analyzed with DNASTAR Lasergene 15.

### 2.10. Statistical Analysis

GraphPad Prism v9 was used to complete all data analysis. Infectivity data shown represent averages of three biological replicates with the standard deviation between the trials. In vivo challenge study data is the average of 5 mice included in each group. Error bars represent the standard deviation at each data point.  $p$  values below 0.05 were considered significant in this study. Statistical analysis of TCID<sub>50</sub> titers was performed through multiple unpaired t-tests using two-tailed  $p$  values, and significant differences in survival were inferred using the log-rank Mantel–Cox to determine differences between groups (\*  $p < 0.05$ , \*\*  $p < 0.01$ ).

## 3. Results

### 3.1. Lethality of Phu/13 and FL/4/06 in Mice Prior to Mouse-Adapting

Influenza viruses do not typically cause disease in mice. However, lethal challenge strains of influenza are often optimal for vaccine and therapeutics studies [26,29,32–34]. Therefore, mouse-adapting is used to produce a disease model for use in laboratory studies [23,26]. Before beginning the mouse-adapting process, we first needed to characterize any pathogenicity these viruses already possessed in mice. TCID<sub>50</sub>/mL virus titers were calculated before challenging female BALB/cJ mice with a 1:2 dilution of chorioallantoic fluid containing either 3.5log<sub>10</sub>TCID<sub>50</sub> units Phu/13 or 5log<sub>10</sub>TCID<sub>50</sub> units FL/4/06 in a 20  $\mu$ L dose (Figure 2A). This was the maximum infectious dose of each virus that could be delivered. Weight loss was monitored for 14 days after infection (Figure 2B). No signs of meaningful weight loss were detected in the two weeks post-challenge with the maximum amount of virus able to be used prior to mouse-adaptation.

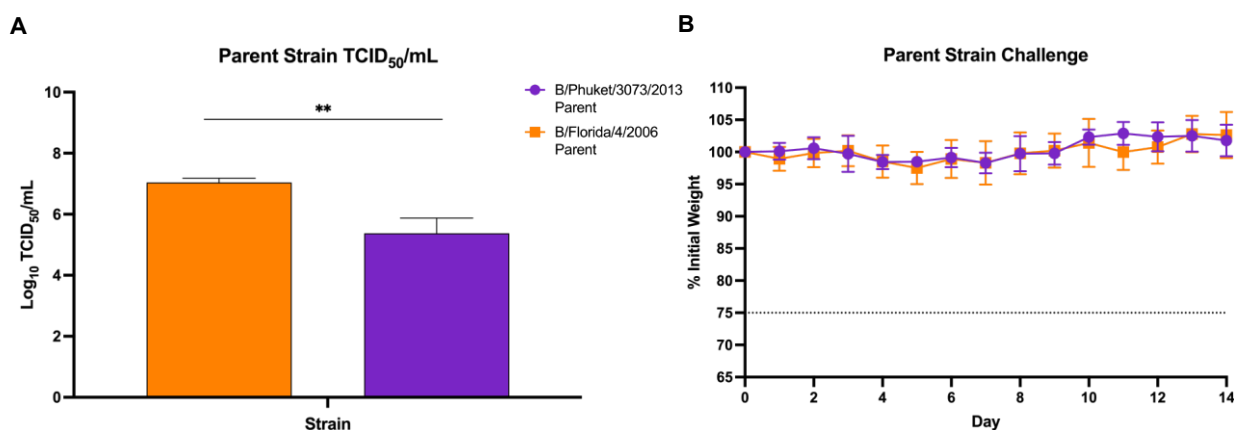


**Figure 2.** Live challenge with wild-type B/Florida/4/2006 and B/Phuket/3073/2013. (A) TCID<sub>50</sub> values for each strain used for initial passage infection. Values shown are an average of three independent experiments with error bars representing standard deviation between three independent replicates. Statistical significance was determined through unpaired  $t$ -test, \*\*  $p < 0.01$ ; (B) Weight loss over 14 days shown after i.n. infection with 1:2 dilution of allantoic fluid of each parent virus. A  $\geq 25\%$  initial weight lost (dotted line) was used as a threshold for humane sacrifice of the animals.

### 3.2. Infectivity of maB/Yam Viruses in Vitro and Lethality in Mice after 10 Passages

To increase lethality for use in challenge studies, serial lung-passaging of these viruses was performed. A detailed schematic is shown (Figure 1). Direct lung-lung passages were performed without an intermediate growth step in between to maintain the virus in the ultimate target setting of the mouse lung. After completion of 10 serial lung-lung passages, the homogenized lung lysate was used to infect both embryonated eggs and MDCK-Ln cell culture to produce large volumes of high-titer viruses for future use. RT-PCR was then used to confirm presence of IBV RNA after expansion (data not shown). The resultant virus stocks were denoted using the strain combined with the passage number and growth medium (p10E or p10C). Before infecting mice with the newly expanded mouse-adapted viruses, we determined in vitro infectivity of the viruses using MDCK-Ln cells (Figure 3A). Both viruses grew to high infectious titers after expansion of virus from the lung lysate. Interestingly, FL/4/06 p10C was less infectious in vitro than p10E despite being grown in the cells used for the infectivity assay (Figure 3A).

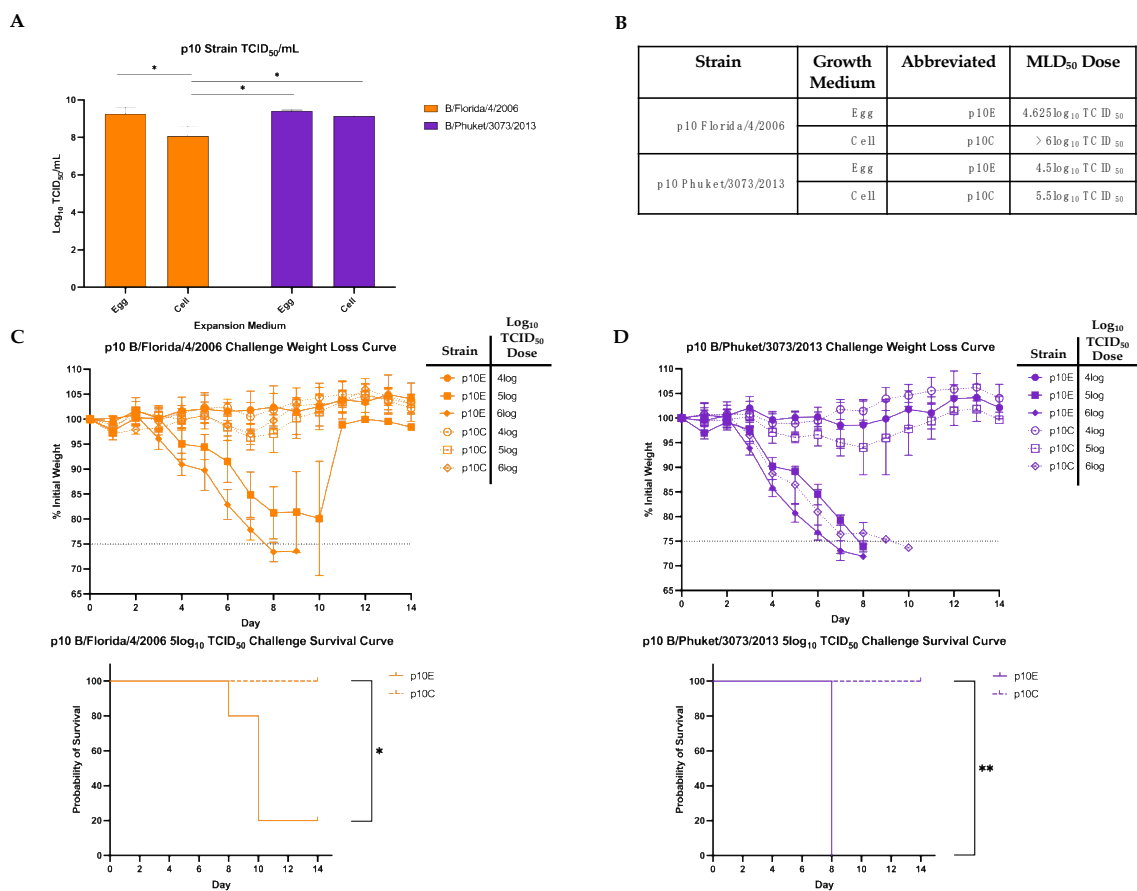


**Figure 3.** Determination of pathogenicity of maB/Yam in mice. (A) TCID<sub>50</sub>/mL titers of both strains after 10 lung-lung passages and expanded in either embryonated eggs (p10E) or MDCK-Ln cell culture (p10C). (B) Table breaking down MLD<sub>50</sub> values calculated using the Reed–Meunch method (31) for each virus strain. (C) Mice challenged with doses corresponding to logTCID<sub>50</sub> of FL/4/06 p10E or p10C were followed for 14 d.p.i. for weight loss (top) and survival after challenge with 5log TCID<sub>50</sub> units (bottom). A ≥25% initial weight lost was used as a threshold for humane sacrifice of the animals. (D) Mice challenged with doses corresponding to logTCID<sub>50</sub> of Phu/13 p10E or p10C were followed for 14 d.p.i. for weight loss (top) and survival after challenge with 5log TCID<sub>50</sub> units (bottom). A ≥25% initial weight lost was used as a threshold for humane sacrifice of the animals. Statistical differences in TCID<sub>50</sub>/mL titers were calculated using unpaired t-tests, while statistical significance between group survival was calculated through log-rank Mantel–Cox test. Statistical analysis was performed in GraphPad Prism 9.0 (\*  $p < 0.05$ , \*\*  $p < 0.01$ ).

Groups of five mice were challenged with p10E or p10C from either strain using the same TCID<sub>50</sub> unit dose to determine if either expansion media conferred higher mortality *in vivo*. Each group was infected with a serial 10-fold dilution starting from 6log<sub>10</sub> TCID<sub>50</sub> units and were monitored for weight loss and mortality. A table of the median lethal dose (MLD<sub>50</sub>) values calculated with the Reed–Muench method [31] is provided (Figure 3B). The full weight loss graph for each MLD<sub>50</sub> is provided (Figure 3C,D). Groups are presented based on whether the virus was grown in eggs (p10E) or in cells (p10C) and the log<sub>10</sub> TCID<sub>50</sub> challenge dose. Weight loss was much more drastic in mice infected with p10E strains down to as low as a 5log<sub>10</sub> TCID<sub>50</sub> unit dose when compared with virus grown in cells. Similar weight loss was observed between p10E and p10C of both FL/06 and Phu/13 at a 4log<sub>10</sub> TCID<sub>50</sub> unit dose, below our calculated MLD<sub>50</sub> values. When we focused on the 5log<sub>10</sub> TCID<sub>50</sub> unit dose, we observed a significant difference in lethality of both FL/06 and Phu/13 p10E when compared to p10C (Figure 3C,D). Together, these results show after 10 serial passages of two different strains of B/Yam, amplification of virally infected lung lysate in eggs produced a significantly more lethal virus in mice compared to the same lung lysate amplified in cell culture.

### 3.3. Infectivity *In Vitro* and Lethality in Mice of FL/4/06 after 10 Additional Passages

We also set out to see what role additional passaging may play on one of our strain's virulence and if it supports our observations from 10 direct lung-lung passages. To do this, the FL/4/06 p10E virus was used to complete another round of 10 lung-lung passages as described above. The egg-passaged virus was chosen due to its higher initial pathogenicity in mice. After an additional 10 passages, the homogenized lung lysate was used to infect embryonated eggs and MDCK-Ln cell culture for viral expansion. TCID<sub>50</sub>/mL values were once again confirmed and used for dosing in the challenges. Again, FL/4/06 p20E grew to a higher infectious titer in MDCK-Ln cell culture than p20C (Figure 4A).

The challenge doses used for p20E and p20C were identical infectious titers to p10E and p10C. MLD<sub>50</sub> calculations were repeated using the p20 strains (Figure 4B). Again, the post-infection weight loss and survival curves (Figure 4C) show that the p20E viruses maintained lethality significantly better after expansion than p20C viruses. Significant weight loss was observed by day 8 in mice infected with the highest doses of p20E while no severe weight loss was observed in mice infected with any dose of p20C. In the 6 log<sub>10</sub> TCID<sub>50</sub> dose, infection with p20E led to significantly more mortality than infection with p20C (Figure 4C). These results corroborate what was seen after 10 passages of both FL/06 and Phu/13. Interestingly, neither p20E nor p20C viruses increased in lethality after 10 additional passages as measured through MLD<sub>50</sub> titers (Figures 3B and 4B). Differences in survival between p10E and p20E were not significant (Figure 4D). This is especially notable because FL/06 p10E was used to start the further 10 passages, and no significant weight loss or lethality was observed after the virus was grown in MDCK-Ln cells. This highlights the potential for further study to understand why this cell culture system is not conducive to the growth of mouse lethal IBV strains.

### 3.4. Sequence Analysis of FL/4/06 HA and NA before and after Mouse-Adapting

To attempt to find any genetic mutations responsible for the lethality differences observed between the parental and mouse-adapted viruses, we sequenced the HA and NA genes of FL/4/06. We chose to sequence this virus since it had been serially passaged 20 total times in mice. We observed that the HA and NA of the p10 and p20 FL/4/06 were identical to the parental virus irrespective of growth system. The four major antigenic sites of the influenza B virus HA are shown (Figure 5A) [35]. The only identifiable difference observed after sequencing was a single nucleotide mutation in the HA sequence (Figure 5B). However, this mutation was silent and did not change the amino acid sequence. The complete HA amino acid and nucleotide sequence alignments are shown in Figures S1 and S2, respectively. A representative NA amino acid sequence alignment from positions 161–320 is shown (Figure 5C). All amino acid sequences were identical to the parental virus prior to



mouse-adapting. The full-length NA amino acid and nucleotide alignments are shown in Figures S1–S4, respectively.

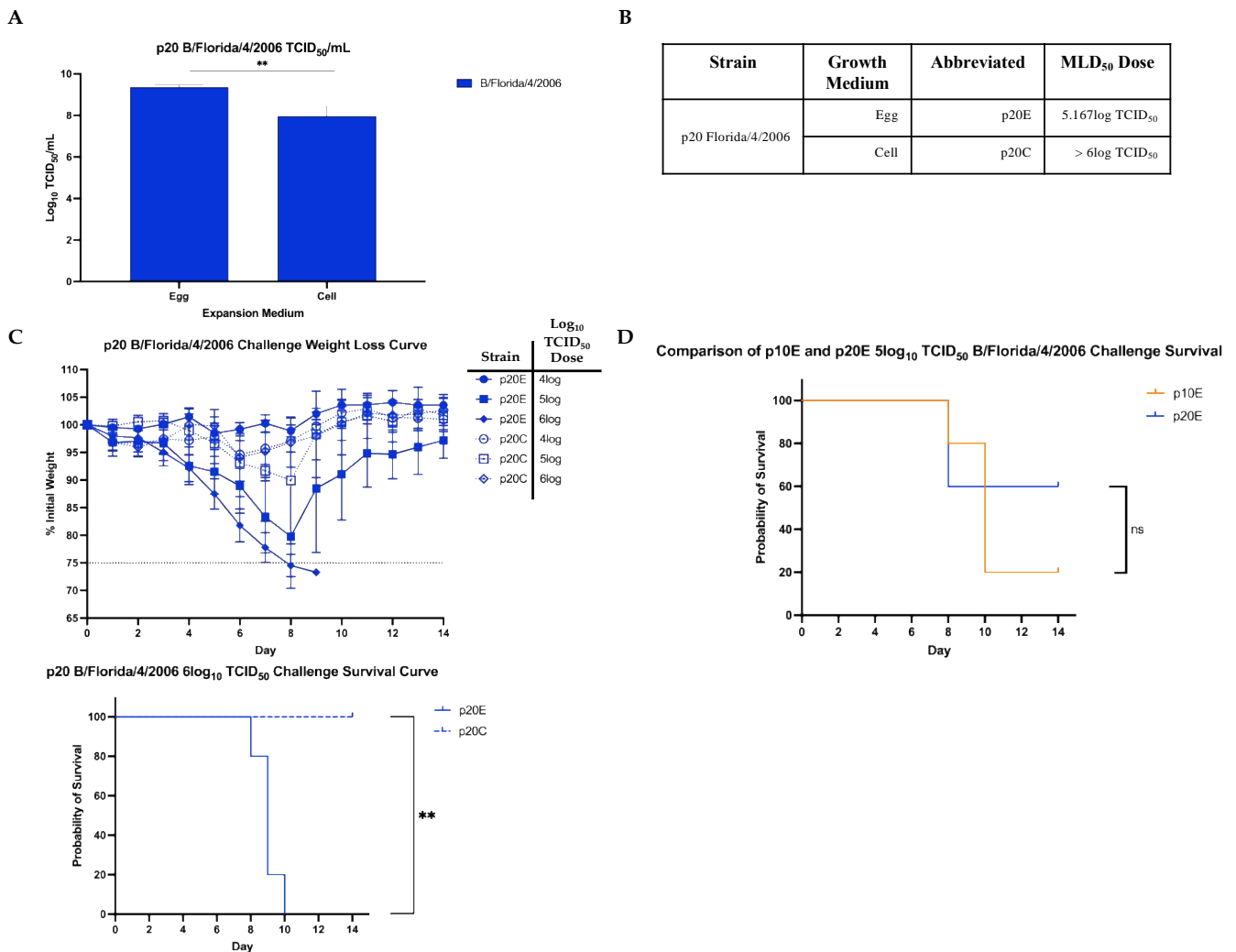


**Figure 4.** Pathogenicity of FL/4/06 after 20 total lung-lung passages. **(A)** TCID<sub>50</sub>/mL titers of FL/4/06 p20E and p20C. **(B)** Table breaking down MLD<sub>50</sub> values calculated using the Reed–Meunch method (31) for FL/4/06 p20E and p20C. **(C)** Mice challenged with doses corresponding to logTCID<sub>50</sub> of FL/4/06 p20E or p20C were followed for 14 d.p.i. for weight loss (top) and survival after challenge with 6log TCID<sub>50</sub> units (bottom). A ≥25% initial weight lost was used as a threshold for humane sacrifice of the animals. **(D)** Comparison of survival probability of mice challenged with 5log TCID<sub>50</sub> of p10E or p20E. No statistically significant difference in survival probability was observed. Statistical differences in TCID<sub>50</sub>/mL titers were calculated using unpaired t-tests, while statistical significance between group survival was calculated through log-rank Mantel–Cox test. Statistical analysis was performed in GraphPad Prism 9.0 \*\*  $p < 0.01$ .

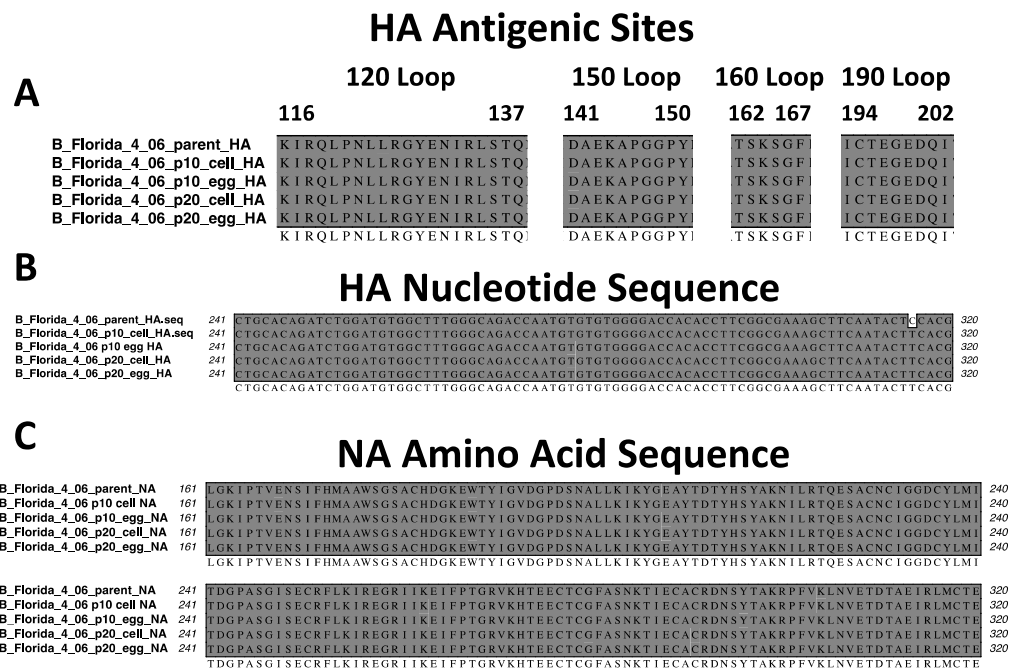


**Figure 5.** FL/4/06 surface glycoprotein sequence analysis. The HA and NA genes were reverse transcribed into cDNA, PCR amplified, and sequenced using Sanger sequencing. (A) The major antigenic sites [35] of the HA protein are shown to be identical to the parental virus. (B) The single nucleotide mutation observed between the parental virus and the mouse-adapted HA sequences was a single silent mutation between nucleotide 241 and 320. (C) A representative amino acid alignment of the NA protein from positions 161–320 shows 100% sequence conservation between the parental and the mouse-adapted viruses.

#### 4. Discussion

Influenza B viruses are relevant respiratory pathogens that cause significant disease burden each year around the globe [1,4–6]. Despite this, the inability to naturally cause infections in many mouse strains has led to difficulty of developing easily accessible small animal disease models for IBV vaccine and therapeutic research. The process of mouse-adapting IBV has been used to define in vivo pathogenic determinants [24–26] and for development of lethal strains for use in vaccine and therapeutics studies [32–34,36]. However, performing mouse-adapting series can be costly and may not produce consistent or repeatable results. Differing genetic determinants of pathogenicity studies in the BALB/c mouse model [23–26] also can contribute to a lack of consistency between procedures. Thus, development of a widely available reverse genetics system for generating lethal viruses such as those for IAV [37,38] is less feasible. Recognizing these issues with the mouse-adapting process, we designed this study to investigate whether growth setting can influence the lethality of IBV after serial lung-lung passaging in mice (Figure 1).

Our results suggest that viral growth system may play a role in mouse-adapted IBV lethality. Having been initially grown in eggs, the parent virus strains showed no lethality in mice over two weeks of infection (Figure 2). These viruses were then passaged 10 times in mice as described above and amplified in both embryonated eggs and MDCK-Ln cells for further study. A total of 10 initial passages were chosen based on previous studies in which mouse-adapted strains of IBV [23] as well as various IAV subtypes were deemed sufficient to increase lethality of the viruses [39,40]. This was also performed more recently for swine influenza H1 viruses [41]. Since 10 passages is often fewer than is required to mouse-adapt IBV [24–26], this served as our benchmark for potential improvement on established methods from the literature. Our model also eliminated any intermediate growth steps in embryonated eggs or MDCK-Ln cell culture in between lung passages. We believed that this may improve pathogenicity at the end after viral growth by maximizing

the amount of time spent in mouse lung tissue and preventing any mutations driven by replication in other systems.

As a proxy for overall pathogenicity, we determined the median lethal dose for the p10 mouse-adapted B/Yam strains grown in eggs and cells. Mice were challenged with equivalent TCID<sub>50</sub> units of each virus (Figure 3). These mice were followed 14 days for weight loss and survival (Figure 3C,D), and the MLD<sub>50</sub> was calculated (Figure 3B). We observed that expanding the final passage lung lysate in eggs led to increased weight loss and significantly lower chance of survival than expansion in MDCK-Ln cell culture for both B/Yam strains. While not often considered in research studies, preparation of mouse-adapted B/Yam stocks appears to play a role in the lethality of these viruses in mice.

To further support our findings, we took one of the two lethal mouse-adapted B/Yam strains and completed a further round of 10 serial lung-lung passages. FL/4/06 p10E was chosen as the initial strain for infection due to its higher initial lethality seen in mice. After 20 total lung-lung passages, the final lung lysate was once again used to infect embryonated eggs or MDCK-Ln cell culture. Infectious titers were obtained in vitro (Figure 4A) and used to calculate challenge doses in mice. Once again, at the same infectious dose, FL/4/06 p20E led to increased weight loss and decreased chance of survival when compared to p20C (Figure 4C). Interestingly, neither p20E nor p20C were able to increase the level of lethality in mice as measured by the MLD<sub>50</sub> titer compared to p10E, the strain used to start further mouse-adapting. While the difference in lethality of p10E and p20E was found to be insignificant (Figure 4D), p20C appeared to lose almost all lethality even after 10 additional passages. This was an unexpected result, but it is possible that the mutations needed to further increase the lethality did not occur in the 10 additional passages. It is also possible that the intermediate egg growth interfered with the ability of these mutations to occur. Additionally, we saw no amino acid mutations in either of the surface glycoproteins even after 20 total serial lung passages. Previous studies have identified mutations across many of the different gene segments, but internal gene mutations are often shown to have the most critical effect on viral pathogenicity [23,24,26]. Further sequencing of the entire viral genome will help elucidate exactly what mutations occurred in our model.

MDCK-Ln cells were chosen for this study due to the increased growth rate and reported increased susceptibility to influenza virus infection with the ability to produce virus at a higher titer than MDCK cells [42,43]. While these strains have both previously been incorporated as influenza vaccine strains, two representative strains may not represent all the diversity in the Yamagata-lineage. More work is required to determine if this phenomenon is shared not only among other strains of B/Yam, but also of B/Vic and ancestral IBV. Another consideration to make is the presence of defective-interfering particles. These particles have been shown to play active roles in modulating host immune responses while also inhibiting replication of normal infectious particles [44]. Our serial lung-lung passage model is unable to rule out production of these particles or highlight what role they could play in the process if these particles are present.

It is also important to recognize egg growth of IBV may not be appropriate for certain studies. Both IBV and IAV have been shown to undergo mutations in the HA which shift receptor-binding capability towards embryonated eggs and away from human epithelial tissue by passaging [45,46]. These egg-adapted mutations also have been shown to alter the antigenicity of the viruses [47]. However, our viral glycoprotein sequence analysis showed that even over 20 lung passages as well as expansion steps in embryonated eggs and/or cell culture, no further mutations occurred in either the HA or NA. This would suggest the single expansion step did not introduce any egg-adaptation mutations after serial lung passaging. This could be impactful for some vaccine development studies to show limited development of egg-adapted mutations using single replication steps rather than repeated egg passage over time. Additionally, if growth of virus in eggs was responsible for lethality, we would have expected to see some mortality in our parent strain challenge at a high concentration of egg-grown virus (Figure 2B). This leads us to conclude that the serial lung-lung passaging played the primary role in the lethality we observed.

In this study, our preliminary findings support that influenza B virus pathogenicity in mice may not require adaptation in the surface glycoproteins to increase lethality. While our results cannot rule out internal gene mutations, any genetic differences between virus grown in eggs and virus grown in cell culture would have been influenced by the growth systems. These different settings appear to be capable of influencing the *in vivo* lethality of mouse-adapted IBV. Further research with our model will better characterize this phenomenon and assist in overcoming a major hurdle in the influenza vaccine and therapeutic research field. By increasing the availability of better disease models, we hope to assist in the development of more suitable tools to study this important disease.

## 5. Conclusions

Influenza B viruses are primarily a human pathogen. While known to cause a significant portion of annual influenza infections and severe disease, development of mouse disease models has historically been difficult and inconsistent. We aimed to identify if the growth system of viral expansion after mouse-adapting influences lethality when used in mouse challenge studies. We used two Yamagata-lineage strains for our mouse-adapting model. Our results show that at the same *in vitro* infectious dose, virus grown in embryonated eggs is significantly more lethal than the same virus grown in MDCK-Ln cell culture. The differences in lethality between virus grown in eggs and cell culture was not due to amino acid changes in the surface glycoprotein sequences. Further studies will aim to identify the mechanism which drives these differences in lethality.

**Supplementary Materials:** The following supporting information can be downloaded at: <https://www.mdpi.com/article/10.3390/v14061299/s1>, Figure S1. Hemagglutinin amino acid sequence alignment of B/Florida/06, Figure S2. Hemagglutinin nucleotide sequence alignment of B/Florida/06, Figure S3. Neuraminidase amino acid sequence alignment of B/Florida/06, Figure S4. Neuraminidase nucleotide sequence alignment of B/Florida/06.

**Author Contributions:** Conceptualization, M.J.P. and E.A.W.; methodology, M.J.P., E.M.P.-T., A.R., R.J.W. and E.A.W.; formal analysis, M.J.P., A.R. and E.A.W.; investigation, M.J.P., E.M.P.-T. and A.R.; resources, R.J.W. and E.A.W.; validation, M.J.P. and E.M.P.-T.; writing—original draft preparation, M.J.P. and E.A.W.; writing—review and editing, M.J.P., E.M.P.-T., A.R., R.J.W. and E.A.W.; visualization, M.J.P. and E.A.W.; supervision, R.J.W. and E.A.W.; project administration, E.A.W.; funding acquisition, E.A.W. All authors have read and agreed to the published version of the manuscript.

**Funding:** This research was supported by the National Institutes of Health (NIH) under Ruth L. Kirschstein National Research Service Award 1 T32 AI125207 and the NIH, National Institute for Allergies and Infectious Diseases (NIAID), grant number R01-AI147109. The funders had no role in data collection and interpretation, or the decision to submit the work for publication.

**Institutional Review Board Statement:** All animal experiments performed in this study were approved by the Institutional Animal Care and Use Committee (IACUC) of the University of Nebraska-Lincoln (protocol #2158, 10/20/2021).

**Informed Consent Statement:** Not applicable.

**Data Availability Statement:** No new data were created or analyzed in this study. Data sharing is not applicable to this article.

**Acknowledgments:** The authors would like to thank [BioRender.com](https://BioRender.com) (22 May 2022) for use of their software for schematic production used in this article.

**Conflicts of Interest:** The authors declare no conflict of interest.

## References

1. World Health Organization. Influenza (Seasonal). Available online: [https://www.who.int/en/news-room/fact-sheets/detail/influenza-\(seasonal\)](https://www.who.int/en/news-room/fact-sheets/detail/influenza-(seasonal)) (accessed on 1 September 2021).
2. Koutsakos, M.; Nguyen, T.H.; Barclay, W.S.; Kedzierska, K. Knowns and unknowns of influenza B viruses. *Futur. Microbiol.* **2016**, *11*, 119–135. [[CrossRef](#)] [[PubMed](#)]
3. Laporte, M.; Stevaert, A.; Raeymaekers, V.; Boogaerts, T.; Nehlmeier, I.; Chiu, W.; Benkheil, M.; Vanaudenaerde, B.; Pöhlmann, S.; Naesens, L. Hemagglutinin Cleavability, Acid Stability, and Temperature Dependence Optimize Influenza B Virus for Replication in Human Airways. *J. Virol.* **2019**, *94*, e01430-19. [[CrossRef](#)] [[PubMed](#)]
4. Caini, S.; Kuszniarz, G.; Garate, V.V.; Wangchuk, S.; Thapa, B.; Júnior, F.J.D.P.; De Almeida, W.A.F.; Njouom, R.; Fasce, R.A.; Bustos, P.; et al. The epidemiological signature of influenza B virus and its B/Victoria and B/Yamagata lineages in the 21st century. *PLoS ONE* **2019**, *14*, e0222381. [[CrossRef](#)] [[PubMed](#)]
5. Chan, P.K.S.; Chan, M.C.W.; Cheung, J.L.K.; Lee, N.; Leung, T.F.; Yeung, A.C.M.; Wong, M.C.S.; Ngai, K.L.K.; Nelson, E.A.S.; Hui, D.S.C. Influenza B Lineage Circulation and Hospitalization Rates in a Subtropical City, Hong Kong, 2000–2010. *Clin. Infect. Dis.* **2012**, *56*, 677–684. [[CrossRef](#)]
6. Borchering, R.K.; Gunning, C.E.; Gokhale, D.V.; Weedop, K.B.; Saeidpour, A.; Brett, T.S.; Rohani, P. Anomalous influenza seasonality in the United States and the emergence of novel influenza B viruses. *Proc. Natl. Acad. Sci. USA* **2021**, *118*, e2012327118. [[CrossRef](#)]
7. Rota, P.A.; Wallis, T.R.; Harmon, M.W.; Rota, J.S.; Kendal, A.P.; Nerome, K. Cocirculation of two distinct evolutionary lineages of influenza type B virus since 1983. *Virology* **1990**, *175*, 59–68. [[CrossRef](#)]
8. Su, S.; Chaves, S.S.; Perez, A.; D’Mello, T.; Kirley, P.D.; Yousey-Hindes, K.; Farley, M.M.; Harris, M.; Sharangpani, R.; Lynfield, R.; et al. Comparing Clinical Characteristics Between Hospitalized Adults With Laboratory-Confirmed Influenza A and B Virus Infection. *Clin. Infect. Dis.* **2014**, *59*, 252–255. [[CrossRef](#)]
9. Zaraket, H.; Hurt, A.C.; Clinch, B.; Barr, L.; Lee, N. Burden of influenza B virus infection and considerations for clinical management. *Antivir. Res.* **2020**, *185*, 104970. [[CrossRef](#)]
10. Shang, M.; Blanton, L.; Brammer, L.; Olsen, S.J.; Fry, A.M. Influenza-Associated Pediatric Deaths in the United States, 2010–2016. *Pediatrics* **2018**, *141*, e20172918. [[CrossRef](#)]
11. Read, J.M.; Zimmer, S.; Vukotich, C.; Schweizer, M.L.; Galloway, D.; Lingle, C.; Yearwood, G.; Calderone, P.; Noble, E.; Quadelacy, T.; et al. Influenza and other respiratory viral infections associated with absence from school among schoolchildren in Pittsburgh, Pennsylvania, USA: A cohort study. *BMC Infect. Dis.* **2021**, *21*, 291. [[CrossRef](#)]
12. Centers for Disease Control and Prevention (CDC). Prevention and control of seasonal influenza with vaccines. Recommendations of the advisory committee on immunization practices—United States, 2013–2014. *MMWR Recomm. Rep.* **2013**, *62*, 1–43.
13. Virk, R.K.; Jayakumar, J.; Mendenhall, I.H.; Moorthy, M.; Lam, P.; Linster, M.; Lim, J.; Lin, C.; Oon, L.L.E.; Lee, H.K.; et al. Divergent evolutionary trajectories of influenza B viruses underlie their contemporaneous epidemic activity. *Proc. Natl. Acad. Sci. USA* **2020**, *117*, 619–628. [[CrossRef](#)] [[PubMed](#)]
14. Suntronwong, N.; Klinfueng, S.; Korkong, S.; Vichaiwattana, P.; Thongmee, T.; Vongpunsawad, S.; Poovorawan, Y. Characterizing genetic and antigenic divergence from vaccine strain of influenza A and B viruses circulating in Thailand, 2017–2020. *Sci. Rep.* **2021**, *11*, 735. [[CrossRef](#)] [[PubMed](#)]
15. Kato-Miyashita, S.; Sakai-Tagawa, Y.; Yamashita, M.; Iwatsuki-Horimoto, K.; Ito, M.; Tokita, A.; Hagiwara, H.; Izumida, N.; Nishino, T.; Wada, N.; et al. Antigenic variants of influenza B viruses isolated in Japan during the 2017–2018 and 2018–2019 influenza seasons. *Infl. Other Respir. Viruses* **2020**, *14*, 311–319. [[CrossRef](#)]
16. Katz, J.M.; Webster, R.G. Efficacy of Inactivated Influenza A Virus (H3N2) Vaccines Grown in Mammalian Cells or Embryonated Eggs. *J. Infect. Dis.* **1989**, *160*, 191–198. [[CrossRef](#)]
17. Lugovtsev, V.Y.; Vodeiko, G.M.; Levandowski, R.A. Mutational pattern of influenza B viruses adapted to high growth replication in embryonated eggs. *Virus Res.* **2005**, *109*, 149–157. [[CrossRef](#)]
18. Gaush, C.R.; Smith, T.F. Replication and Plaque Assay of Influenza Virus in an Established Line of Canine Kidney Cells. *Appl. Microbiol.* **1968**, *16*, 588–594. [[CrossRef](#)]
19. Audsley, J.M.; Tannock, G.A. Cell-Based Influenza Vaccines. *Drugs* **2008**, *68*, 1483–1491. [[CrossRef](#)]
20. Barr, I.G.; Donis, R.O.; Katz, J.M.; McCauley, J.W.; Odagiri, T.; Trusheim, H.; Tsai, T.F.; Wentworth, D.E. Cell culture-derived influenza vaccines in the severe 2017–2018 epidemic season: A step towards improved influenza vaccine effectiveness. *NPJ Vaccines* **2018**, *3*, 44. [[CrossRef](#)]
21. Henry, C.; Palm, A.-K.E.; Utset, H.A.; Huang, M.; Ho, I.Y.; Zheng, N.-Y.; Fitzgerald, T.; Neu, K.E.; Chen, Y.-Q.; Krammer, F.; et al. Monoclonal Antibody Responses after Recombinant Hemagglutinin Vaccine versus Subunit Inactivated Influenza Virus Vaccine: A Comparative Study. *J. Virol.* **2019**, *93*, e01150-19. [[CrossRef](#)]
22. Hirst, G.K. Studies on the mechanism of adaptation of influenza virus to mice. *J. Exp. Med.* **1947**, *86*, 357–366. [[CrossRef](#)] [[PubMed](#)]
23. Bae, J.-Y.; Lee, I.; Kim, J.I.; Park, S.; Yoo, K.; Park, M.; Kim, G.; Park, M.S.; Lee, J.-Y.; Kang, C.; et al. A Single Amino Acid in the Polymerase Acidic Protein Determines the Pathogenicity of Influenza B Viruses. *J. Virol.* **2018**, *92*, e00259-18. [[CrossRef](#)] [[PubMed](#)]
24. McCullers, J.A.; Hoffmann, E.; Huber, V.C.; Nickerson, A.D. A single amino acid change in the C-terminal domain of the matrix protein M1 of influenza B virus confers mouse adaptation and virulence. *Virology* **2005**, *336*, 318–326. [[CrossRef](#)] [[PubMed](#)]

25. Prokopyeva, E.; Kurskaya, O.; Sobolev, I.; Solomatina, M.; Murashkina, T.; Suvorova, A.; Alekseev, A.; Danilenko, D.; Komissarov, A.; Fadeev, A.; et al. Experimental Infection Using Mouse-Adapted Influenza B Virus in a Mouse Model. *Viruses* **2020**, *12*, 470. [CrossRef] [PubMed]
26. Kim, E.-H.; Park, S.-J.; Kwon, H.-I.; Kim, S.M.; Kim, Y.-I.; Song, M.-S.; Choi, E.-J.; Pascua, P.N.Q.; Choi, Y.-K. Mouse adaptation of influenza B virus increases replication in the upper respiratory tract and results in droplet transmissibility in ferrets. *Sci. Rep.* **2015**, *5*, 15940. [CrossRef]
27. Bouvier, N.M.; Lowen, A.C. Animal Models for Influenza Virus Pathogenesis and Transmission. *Viruses* **2010**, *2*, 1530–1563. [CrossRef]
28. Okuno, Y.; Matsumoto, K.; Isegawa, Y.; Ueda, S. Protection against the mouse-adapted A/FM/1/47 strain of influenza A virus in mice by a monoclonal antibody with cross-neutralizing activity among H1 and H2 strains. *J. Virol.* **1994**, *68*, 517–520. [CrossRef]
29. Bullard, B.L.; Corder, B.N.; DeBeauchamp, J.; Rubrum, A.; Korber, B.; Webby, R.J.; Weaver, E.A. Epigraph hemagglutinin vaccine induces broad cross-reactive immunity against swine H3 influenza virus. *Nat. Commun.* **2021**, *12*, 1203. [CrossRef]
30. World Health Organization Global Influenza Surveillance Network. Manual for the Laboratory Diagnosis and Virological Surveillance of Influenza. Available online: [https://apps.who.int/iris/bitstream/handle/10665/44518/9789241548090\\_eng.pdf;jsessionid=BE6CFCB2A97A79537B02FA59ADB3BE98?sequence=1](https://apps.who.int/iris/bitstream/handle/10665/44518/9789241548090_eng.pdf;jsessionid=BE6CFCB2A97A79537B02FA59ADB3BE98?sequence=1) (accessed on 9 September 2021).
31. Reed, L.J.; Muench, H.A. A simple method for estimating fifty percent endpoints. *Am. J. Hyg.* **1938**, *27*, 493–497.
32. Mo, J.; Cardenas-Garcia, S.; Santos, J.; Ferreri, L.; Cáceres, C.; Geiger, G.; Perez, D.; Rajao, D. Mutation E48K in PB1 Polymerase Subunit Improves Stability of a Candidate Live Attenuated Influenza B Virus Vaccine. *Vaccines* **2021**, *9*, 800. [CrossRef]
33. Shen, C.; Chen, J.; Li, R.; Zhang, M.; Wang, G.; Stegalkina, S.; Zhang, L.; Chen, J.; Cao, J.; Bi, X.; et al. A multimechanistic antibody targeting the receptor binding site potently cross-protects against influenza B viruses. *Sci. Transl. Med.* **2017**, *9*, eaam5752. [CrossRef]
34. Abed, Y.; Fage, C.; Checkmahomed, L.; Venable, M.-C.; Boivin, G. Characterization of contemporary influenza B recombinant viruses harboring mutations of reduced susceptibility to baloxavir marboxil, in vitro and in mice. *Antivir. Res.* **2020**, *179*, 104807. [CrossRef] [PubMed]
35. Wang, Q.; Cheng, F.; Lu, M.; Tian, X.; Ma, J. Crystal Structure of Unliganded Influenza B Virus Hemagglutinin. *J. Virol.* **2008**, *82*, 3011–3020. [CrossRef] [PubMed]
36. Liu, Y.; Strohmeier, S.; González-Domínguez, I.; Tan, J.; Simon, V.; Krammer, F.; García-Sastre, A.; Palese, P.; Sun, W. Mosaic Hemagglutinin-Based Whole Inactivated Virus Vaccines Induce Broad Protection Against Influenza B Virus Challenge in Mice. *Front. Immunol.* **2021**, *12*, 746447. [CrossRef] [PubMed]
37. Kobasa, D.; Takada, A.; Shinya, K.; Hatta, M.; Halfmann, P.; Theriault, S.; Suzuki, H.; Nishimura, H.; Mitamura, K.; Sugaya, N.; et al. Enhanced virulence of influenza A viruses with the haemagglutinin of the 1918 pandemic virus. *Nature* **2004**, *431*, 703–707. [CrossRef]
38. Blazejewska, P.; Koscinski, L.; Viegas, N.; Anhlan, D.; Ludwig, S.; Schughart, K. Pathogenicity of different PR8 influenza A virus variants in mice is determined by both viral and host factors. *Virology* **2011**, *412*, 36–45. [CrossRef]
39. Zhang, C.; Zhao, Z.; Guo, Z.; Zhang, J.; Li, J.; Yang, Y.; Lu, S.; Wang, Z.; Zhi, M.; Fu, Y.; et al. Amino Acid Substitutions Associated with Avian H5N6 Influenza A Virus Adaptation to Mice. *Front. Microbiol.* **2017**, *8*, 1763. [CrossRef]
40. Slaine, P.D.; MacRae, C.; Kleer, M.; Lamoureux, E.; McAlpine, S.; Warhuus, M.; Comeau, A.M.; McCormick, C.; Hatchette, T.; Khapersky, D.A. Adaptive Mutations in Influenza A/California/07/2009 Enhance Polymerase Activity and Infectious Virion Production. *Viruses* **2018**, *10*, 272. [CrossRef]
41. Hu, J.; Hu, Z.; Wei, Y.; Zhang, M.; Wang, S.; Tong, Q.; Sun, H.; Pu, J.; Liu, J.; Sun, Y. Mutations in PB2 and HA are crucial for the increased virulence and transmissibility of H1N1 swine influenza virus in mammalian models. *Veter Microbiol.* **2021**, *265*, 109314. [CrossRef]
42. Tsai, H.-C.; Lehman, C.W.; Lin, C.-C.; Tsai, S.-W.; Chen, C.-M. Functional evaluation for adequacy of MDCK-lineage cells in influenza research. *BMC Res. Notes* **2019**, *12*, 101. [CrossRef]
43. Lin, S.-C.; Kappes, M.A.; Chen, M.-C.; Lin, C.-C.; Wang, T.T. Distinct susceptibility and applicability of MDCK derivatives for influenza virus research. *PLoS ONE* **2017**, *12*, e0172299. [CrossRef] [PubMed]
44. Ghorbani, A.; Ngunjiri, J.M.; Lee, C.-W. Influenza A Virus Subpopulations and Their Implication in Pathogenesis and Vaccine Development. *Annu. Rev. Anim. Biosci.* **2020**, *8*, 247–267. [CrossRef] [PubMed]
45. Gambaryan, A.; Robertson, J.; Matrosovich, M. Effects of Egg-Adaptation on the Receptor-Binding Properties of Human Influenza A and B Viruses. *Virology* **1999**, *258*, 232–239. [CrossRef] [PubMed]
46. Powell, H.; Liu, H.; Pekosz, A. Changes in sialic acid binding associated with egg adaptation decrease live attenuated influenza virus replication in human nasal epithelial cell cultures. *Vaccine* **2021**, *39*, 3225–3235. [CrossRef] [PubMed]
47. Saito, T.; Nakaya, Y.; Suzuki, T.; Ito, R.; Saito, T.; Saito, H.; Takao, S.; Sahara, K.; Odagiri, T.; Murata, T.; et al. Antigenic alteration of influenza B virus associated with loss of a glycosylation site due to host-cell adaptation. *J. Med. Virol.* **2004**, *74*, 336–343. [CrossRef]